# Online Appendix

## Reading the Future of Oil: A Noncausal Approach to Supply News Shocks

Stéphane Auray[a] Zakaria Moussa[b] Arthur Thomas[c]

[a]CREST-Ensai and Rennes School of Business

[b]Nantes University, LEMNA, France

[c]Université Paris-Dauphine, Université PSL, LEDa, CNRS, IRD, 75016 Paris, France

---

This Online Appendix accompanies the main paper and is organized as follows. Appendix A clarifies the relationship between the multiplicative VMAR$(r, s)$ representation and the alternative VAR$(n_1, n_2, p)$ framework of Davis and Song (2020) and Gourieroux and Jasiak (2017), and shows that the rank conditions required for equivalence fail in our setting. Appendix B extends the stylised news model to an arbitrary anticipation horizon $l$ and formally establishes recoverability of the oil supply news shock in the sense of Chahrour and Jurado (2021). Appendix C describes all data series used in the empirical analysis together with their sources and transformations. Appendix D provides a self-contained account of the Bayesian Gibbs sampler used to estimate the NC-VAR$(r, s)$ model. Appendix E gathers validation evidence for the noncausal specification, including the posterior distribution of the degrees-of-freedom parameter and the lag/lead selection procedure. Appendices G–F report additional impulse responses and historical decompositions, including the OPEC/Non-OPEC disaggregation and a comparison of causal versus noncausal estimates.

# A Equivalence with alternative NC-VAR specifications

This appendix clarifies how the multiplicative VMAR$(r, s)$ representation used in the main text relates to the alternative VAR$(n_1, n_2, p)$ framework of Davis and Song (2020) and Gourieroux and Jasiak (2017). Following Lanne and Saikkonen (2013), the VMAR$(r, s)$ specification underlying equation (7) can, in principle, be recast as a VAR with both stable and unstable roots when certain rank conditions are satisfied. The purpose of this section is to show that these conditions fail in our setting, so that the process $(q_t, p_t)'$ does not admit a VAR$(n_1, n_2, p)$ representation with i.i.d. innovations in the sense of Davis and Song (2020).

The VAR$(n_1, n_2, p)$ representation considered by Davis and Song (2020) and Gourieroux and Jasiak (2017) writes the $n$-dimensional process $y_t$ as

$$y_t = \Theta_1 y_{t-1} + \Theta_2 y_{t-2} + \cdots + \Theta_p y_{t-p} + u_t,$$

where the characteristic polynomial

$$\det\left(I_n - \Theta_1 z - \cdots - \Theta_p z^p\right) = 0$$

has $n_1$ roots outside and $n_2$ roots inside the unit circle, with $n_1 + n_2 = np$. As discussed in Chapter 4 of Giancaterini (2023), the equivalence between this VAR$(n_1, n_2, p)$ representation and the multiplicative VMAR$(r, s)$ form requires, among other things, that the highest-order lead coefficient matrix in the noncausal polynomial have full rank. Intuitively, the noncausal part must be rich enough to generate a full-dimensional unstable block in the companion form.

In our VMAR$(1, 2)$ specification, the noncausal polynomial is

$$\Phi(L^{-1}) = I_2 - \Phi_1 L^{-1} - \Phi_2 L^{-2},$$

with coefficient matrices

$$\Phi_1 = \begin{bmatrix} 0 & 0 \\ -\beta & 0 \end{bmatrix}, \qquad \Phi_2 = \begin{bmatrix} 0 & 0 \\ -\dfrac{\beta^2}{1-\rho\beta} & 0 \end{bmatrix}.$$

The highest-order lead coefficient $\Phi_2$ is clearly rank-deficient. Computing its determinant gives

$$\det(\Phi_2) = \det \begin{bmatrix} 0 & 0 \\ -\dfrac{\beta^2}{1-\rho\beta} & 0 \end{bmatrix} = 0 \times 0 - 0 \times \left(-\frac{\beta^2}{1-\rho\beta}\right) = 0, \tag{A1}$$

so that $\text{rank}(\Phi_2) = 1 < 2 = n$. The full-rank requirement of Giancaterini (2023) is therefore violated.

This rank deficiency is not merely an algebraic curiosity; it has structural implications. It reflects the triangular transmission mechanism of news shocks in our model, whereby production remains purely backward-looking, while prices load on future production through the lead terms. In the noncausal polynomial, this structure manifests itself in a lead block that does not span the full two-dimensional space, thereby preventing the construction of a VAR$(n_1, n_2, p)$ representation with a non-singular unstable block and i.i.d. innovations in the sense of Davis and Song (2020) and Gourieroux and Jasiak (2017).

The point can be seen even more transparently by considering the companion form of the noncausal component. Define the stacked process $Z_t = (y_t', y_{t+1}')'$ and rewrite the noncausal part as

$$Z_t = \Upsilon Z_{t+1} + v_t,$$

where the companion matrix $\Upsilon$ is given by

$$\Upsilon = \begin{bmatrix} \Phi_1 & \Phi_2 \\ I_2 & 0 \end{bmatrix} = \begin{bmatrix} 0 & 0 & 0 & 0 \\ -\beta & 0 & -\dfrac{\beta^2}{1-\rho\beta} & 0 \\ 1 & 0 & 0 & 0 \\ 0 & 1 & 0 & 0 \end{bmatrix}. \tag{A2}$$

Because $\Phi_2$ is rank-deficient, $\Upsilon$ is singular, and the eigenvalue decomposition required to separate stable and unstable blocks in the Gourieroux and Jasiak (2017) representation theorem cannot be implemented in the standard way. In particular, one cannot construct a full set of eigenvectors that span the state space and correspond to a VAR$(n_1, n_2, p)$ process with an i.i.d. innovation vector.

Importantly, this rank deficiency does not undermine the validity of our approach. The multiplicative VMAR$(r, s)$ representation of Lanne and Saikkonen (2013) remains well defined and estimable, because both the causal and noncausal polynomials satisfy the usual stability conditions, $\det \Pi(z) \neq 0$ and $\det \Phi(z) \neq 0$ for $|z| \leq 1$. The failure of the full-rank condition simply indicates that our NC-VAR lies outside the class of VAR$(n_1, n_2, p)$ models considered by Davis and Song (2020) and Gourieroux and Jasiak (2017), owing to the triangular structure imposed by the economic model. As shown in the main text, recoverability of the structural shocks, in the sense of Chahrour and Jurado (2021), remains fully intact within the VMAR framework.

# B Noncausal representation and recoverability in the general news model

This appendix extends the stylised model of Section 2 to a more general specification of the oil production process with news shocks, following Nelimarkka (2017a). We derive the NC-VAR$(1, l)$ representation for arbitrary anticipation horizon $l \geq 1$ and establish recoverability of the oil supply news shock in the sense of Chahrour and Jurado (2021). The analysis highlights how the noncausal structure arises from the interaction of forward-looking pricing and lagged effects of news on production, and clarifies the conditions under which the structural shocks can be recovered from observables.

## B.1 General oil production process with news

Consider the general oil production process

$$q_t = \rho q_{t-1} + \chi \epsilon_t + \epsilon_{t-l}, \tag{A3}$$

where $|\rho| < 1$, $l \geq 1$ denotes the anticipation horizon, and $\chi \in [0, 1)$ measures the contemporaneous impact of the news shock on production. When $\chi = 0$, the news shock is purely anticipatory and affects production only with a delay of $l$ periods; when $0 < \chi < 1$, the shock has both contemporaneous and lagged effects, but the anticipated component still dominates. The real price of oil, or any forward-looking variable such as inventories in the absence of capacity constraints, is determined by the forward-looking equilibrium condition

$$p_t = \beta \mathbb{E}_t[p_{t+1}] - q_t + \nu_t, \tag{A4}$$

where $|\beta| < 1$ and $\nu_t$ is an exogenous price disturbance orthogonal to $\epsilon_t$. The negative sign reflects the inverse relationship between supply and price: higher supply depresses the equilibrium price, holding demand and expectations constant. Solving (A4) forward yields

$$p_t = -\sum_{j=0}^{\infty} \beta^j \mathbb{E}_t[q_{t+j}] + \nu_t, \tag{A5}$$

so that the price at time $t$ is the present value of expected future production, up to the disturbance $\nu_t$.

Iterating (A3) forward gives, for $j \geq 1$,

$$q_{t+j} = \rho^j q_t + \sum_{i=0}^{j-1} \rho^{j-1-i} \Big( \chi \epsilon_{t+1+i} + \epsilon_{t+1+i-l} \Big). \tag{A6}$$

Taking conditional expectations and using $\mathbb{E}_t[\epsilon_{t+k}] = \epsilon_{t+k}$ for $k \leq 0$ and $\mathbb{E}_t[\epsilon_{t+k}] = 0$ for

$k > 0$, we obtain, for $j \geq 1$,

$$\mathbb{E}_t[q_{t+j}] = \rho^j q_t + \sum_{i=0}^{\min(j-1,\, l-1)} \rho^{j-1-i} \epsilon_{t+1+i-l}. \tag{A7}$$

Re-indexing the second term by setting $k = l - 1 - i$, so that $\epsilon_{t+1+i-l} = \epsilon_{t-k}$, yields

$$\mathbb{E}_t[q_{t+j}] = \rho^j q_t + \sum_{k=\max(l-j,0)}^{l-1} \rho^{j-l+k} \epsilon_{t-k}, \qquad j \geq 1. \tag{A8}$$

**Proposition A1.** *Suppose $|\rho| < 1$, $|\beta| < 1$ and $\chi \in [0, 1)$. Then the equilibrium price $p_t$ in (A5) can be written as*

$$p_t = -\theta\rho q_{t-1} - \sum_{k=0}^{l} \gamma_k \epsilon_{t-k} + \nu_t, \tag{A9}$$

*where $\theta = (1 - \rho\beta)^{-1}$ and the coefficients $\gamma_k$ are given by*

$$\gamma_0 = \theta(\chi + \beta^l), \tag{A10}$$

$$\gamma_k = \theta\beta^{l-k}, \qquad 1 \leq k \leq l - 1, \tag{A11}$$

$$\gamma_l = \theta. \tag{A12}$$

*Proof.* Substituting (A8) into (A5), we separate the contribution of current production from that of the news shocks. The contribution of the current fundamental component is

$$-\sum_{j=0}^{\infty} \beta^j \rho^j q_t = -\frac{1}{1 - \rho\beta} q_t = -\theta q_t.$$

Using $q_t = \rho q_{t-1} + \chi\epsilon_t + \epsilon_{t-l}$, this term becomes

$$-\theta q_t = -\theta\rho q_{t-1} - \theta\chi\epsilon_t - \theta\epsilon_{t-l}.$$

The anticipatory component arises from the second term in (A8), which yields, for each $k \in \{0, \ldots, l - 1\}$,

$$-\sum_{j=1}^{\infty} \beta^j \sum_{k=\max(l-j,0)}^{l-1} \rho^{j-l+k} \epsilon_{t-k}.$$

For a given $k$, the sums over $j$ start at $j = l - k$, so

$$\sum_{j=l-k}^{\infty} \beta^j \rho^{j-l+k} = (\rho\beta)^{l-k} \sum_{j=l-k}^{\infty} (\rho\beta)^{j-(l-k)} = \frac{(\rho\beta)^{l-k}}{1 - \rho\beta} = \theta\beta^{l-k}.$$

Thus $\epsilon_{t-k}$ receives an additional coefficient $\theta\beta^{l-k}$ from anticipation for $k \in \{0, \ldots, l - 1\}$. Combining the fundamental and anticipatory contributions, $\epsilon_t$ receives $\theta\chi$ from the

fundamental part and $\theta\beta^l$ from anticipation, for a total coefficient $\gamma_0 = \theta(\chi + \beta^l)$; the intermediate shocks $\epsilon_{t-k}$ for $1 \le k \le l-1$ receive only the anticipatory term with coefficient $\gamma_k = \theta\beta^{l-k}$; and $\epsilon_{t-l}$ receives $\theta$ from the fundamental part and no anticipatory contribution, so $\gamma_l = \theta$. Substituting these coefficients yields (A9). □

Specialising to a two-period anticipation horizon $l = 2$ reproduces the expression used in the main text: $\gamma_0 = \theta(\chi + \beta^2)$, $\gamma_1 = \theta\beta$, $\gamma_2 = \theta$, and

$$p_t = -\theta\rho q_{t-1} - \theta(\chi + \beta^2)\epsilon_t - \theta\beta\epsilon_{t-1} - \theta\epsilon_{t-2} + \nu_t. \tag{A13}$$

## B.2 Moving-average representation and non-fundamentalness

The joint dynamics of $y_t = (q_t, p_t)'$ can be written as

$$y_t = \begin{bmatrix} \rho & 0 \\ -\theta\rho & 0 \end{bmatrix} y_{t-1} + B(L) \begin{bmatrix} \epsilon_t \\ \nu_t \end{bmatrix}, \tag{A14}$$

where the moving-average polynomial $B(L)$ has the triangular form

$$B(L) = \begin{bmatrix} \chi + L^l & 0 \\ -b_{21}(L) & 1 \end{bmatrix}, \tag{A15}$$

with

$$b_{21}(L) = \gamma_0 + \sum_{k=1}^{l-1} \gamma_k L^k + \gamma_l L^l.$$

**Lemma A1.** *The moving-average representation (A14) is non-fundamental if and only if $\chi < 1$. The determinant polynomial is*

$$\det B(z) = \chi + z^l, \tag{A16}$$

*which has $l$ roots*

$$z_k = \chi^{1/l} \exp\Big(i\pi(2k+1)/l\Big), \qquad k = 0, 1, \ldots, l-1, \tag{A17}$$

*all with modulus $|z_k| = \chi^{1/l} < 1$ whenever $\chi < 1$.*

*Proof.* The triangular structure of $B(z)$ implies

$$\det B(z) = (\chi + z^l) \cdot 1 = \chi + z^l.$$

Setting $\det B(z) = 0$ yields $z^l = -\chi = \chi e^{i\pi}$. The $l$ complex roots are

$$z_k = \chi^{1/l} \exp\Big(i\pi(2k+1)/l\Big), \qquad k = 0, \ldots, l-1,$$

each with modulus $|z_k| = \chi^{1/l}$. For $\chi < 1$, all roots lie strictly inside the unit circle, so the moving-average polynomial is not invertible on the closed unit disc and the representation is non-fundamental. □

The roots $\{z_k\}$ are uniformly distributed on a circle of radius $\chi^{1/l}$ centred at the origin, with angular separation $2\pi/l$. For $l = 2$, they are $\pm i\sqrt{\chi}$; for $l = 3$, they lie at angles $\pi/3$, $\pi$ and $5\pi/3$, and so on. Thus, as soon as the anticipated component dominates ($\chi < 1$), non-fundamentalness arises.

## B.3 Noncausal representation of the general news model

To address non-fundamentalness, we reformulate the model in noncausal form. Starting from (A3), we write

$$(1 - \rho L)q_t = (\chi + L^l)\epsilon_t.$$

The right-hand side can be expressed using lead operators by factoring out $L^l$:

$$(\chi + L^l)\epsilon_t = L^l(\chi L^{-l} + 1)\epsilon_t = (1 + \chi L^{-l})\epsilon_{t-l}.$$

**Lemma A2.** *If $\chi < 1$, the polynomial $1 + \chi z^l$ has all its roots outside the unit circle. Consequently, $1 + \chi L^{-l}$ is invertible on the unit circle.*

*Proof.* The roots of $1 + \chi z^l = 0$ are

$$z_k = \chi^{-1/l} \exp\Big(i\pi(2k + 1)/l\Big), \qquad k = 0, \dots, l - 1,$$

with modulus $|z_k| = \chi^{-1/l} > 1$ whenever $\chi < 1$. Hence all roots lie outside the unit circle, and the polynomial is invertible for $|z| \leq 1$. □

Using Lemma A2, we obtain

$$(1 - \rho L)(1 + \chi L^{-l})^{-1} q_t = \epsilon_{t-l}. \tag{A18}$$

The inverse $(1 + \chi L^{-l})^{-1}$ admits the power-series expansion

$$(1 + \chi L^{-l})^{-1} = \sum_{j=0}^{\infty} (-\chi)^j L^{-lj},$$

so that $q_t$ depends on a (possibly infinite) number of future values of $\epsilon_{t-l}$. Substituting into the price equation produces a noncausal VAR of order $(1, l)$.

**Proposition A2.** *Suppose* $|\rho| < 1$, $|\beta| < 1$ *and* $0 \leq \chi < 1$. *Then the system* (A3)–(A4) *admits a NC-VAR*$(1, l)$ *representation*

$$\Pi(L)\Phi(L^{-1})y_t = B_0 u_t, \tag{A19}$$

*where* $y_t = (q_t, p_t)'$, $u_t = (\epsilon_{t-l}, \nu_t)'$, *and*

$$\Pi(L) = I_2 - \Pi_1 L, \qquad \Pi_1 = \begin{bmatrix} \rho & 0 \\ -\theta\rho & 0 \end{bmatrix}, \tag{A20}$$

$$\Phi(L^{-1}) = I_2 - \sum_{j=1}^{s} \Phi_j L^{-j}, \qquad \Phi_j = \begin{bmatrix} \phi_{j,11} & 0 \\ \phi_{j,21} & 0 \end{bmatrix}, \tag{A21}$$

$$B_0 = \begin{bmatrix} 1 & 0 \\ -1 & 1 \end{bmatrix}. \tag{A22}$$

*The lead coefficients* $\phi_{j,11}$ *and* $\phi_{j,21}$ *depend on* $\chi$ *and* $l$ *as follows:*

1. *If* $\chi = 0$ *(pure news shock), the noncausal polynomial is finite and the truncation order is* $s = l$. *The upper-left element of each lead matrix vanishes,* $\phi_{j,11} = 0$ *for all* $j \geq 1$, *while the lower-left elements satisfy* $\phi_{1,21} = -\beta$, $\phi_{l,21} = -\theta(\chi + \beta^l)$ *evaluated at* $\chi = 0$, *and* $\phi_{j,21} = 0$ *otherwise.*

2. *If* $0 < \chi < 1$ *(mixed shocks), the expansion* $(1 + \chi L^{-l})^{-1} = \sum_{k=0}^{\infty} (-\chi)^k L^{-kl}$ *implies that non-zero entries in* $\phi_{j,11}$ *occur only at multiples of* $l$*:*

$$\phi_{kl,11} = -(-\chi)^k, \qquad k = 1, 2, \ldots.$$

   *In practice, a truncation order* $s \gg l$ *delivers an accurate approximation to the infinite-order noncausal polynomial.*

3. *For the two-period anticipation case* $l = 2$ *with* $0 < \chi < 1$, *the coefficients satisfy*

$$\phi_{j,11} = \begin{cases} 0, & j \text{ odd}, \\ -(-\chi)^{j/2}, & j \text{ even}, \end{cases} \tag{A23}$$

$$\phi_{j,21} = \begin{cases} -\beta(-\chi)^{(j-1)/2}, & j \text{ odd}, \\ -\theta(\chi + \beta^2)(- & \\ chi)^{j/2-1}, & j \text{ even}. \end{cases} \tag{A24}$$

*The impulse response coefficients* $\{\Psi_j\}$ *of the two-sided moving-average representation*

*solve the recursion*

$$\Psi_j = \mathbf{1}_{\{j\geq 0\}}\Pi_1^j + \sum_{k=1}^{s} \Phi_k \Psi_{j+k}, \tag{A25}$$

*with boundary condition* $\Psi_j = 0$ *for* $j < -s$.

The proposition shows that the general news model can always be written as a NC-VAR$(1, l)$ process with a finite-order noncausal polynomial when $\chi = 0$ and an infinite-order polynomial when $0 < \chi < 1$, which can be approximated by truncation. The lead structure is lower triangular: production remains backward-looking, while prices inherit the noncausal terms through the lower-left block of $\Phi(L^{-1})$.

## B.4 Recoverability in the sense of Chahrour and Jurado (2021)

We now establish that the structural shocks of the NC-VAR$(1, l)$ representation are recoverable from the observable process in the sense of Chahrour and Jurado (2021). To fix notation, let $\{y_t\}$ be generated from structural shocks $\{u_t\}$ by a linear transformation with spectral characteristic $\varphi(\lambda)$:

$$y_t = \int_{-\pi}^{\pi} e^{i\lambda t}\varphi(\lambda)\Phi_u(d\lambda),$$

where $\Phi_u$ denotes the spectral measure of the shocks.

**Definition A1.** *Chahrour and Jurado (2021). The vector of shocks* $u_t$ *is said to be recoverable from* $\{y_t\}$ *if and only if*

$$\operatorname{rank}\Big[\varphi(\lambda)\Big] = n_u \quad \textit{for almost all } \lambda \in [-\pi, \pi],$$

*where* $n_u$ *is the dimension of* $u_t$.

**Proposition A3.** *Consider the NC-VAR*$(1, l)$ *representation* (A19) *under the following assumptions:*

*(A1)* $|\rho| < 1$ *(stationarity of oil production),*

*(A2)* $|\beta| < 1$ *(convergence of the forward-looking solution),*

*(A3)* $0 \leq \chi < 1$ *(dominance of the anticipated component),*

*(A4)* $l \geq 1$ *(positive anticipation horizon).*

*Then the structural shocks* $u_t = (\epsilon_{t-l}, \nu_t)'$ *are recoverable from the observables* $y_t = (q_t, p_t)'$ *in the sense of Definition A1.*

*Proof.* The NC-VAR$(1, l)$ representation (A19) implies the two-sided moving-average form

$$y_t = \Phi(L^{-1})^{-1}\Pi(L)^{-1}B_0 u_t,$$

with spectral characteristic

$$\varphi(\lambda) = \Phi(e^{i\lambda})^{-1}\Pi(e^{-i\lambda})^{-1}B_0.$$

We show that $\det[\varphi(\lambda)] \neq 0$ for all $\lambda \in [-\pi, \pi]$. The determinant factorises as

$$\det[\varphi(\lambda)] = \frac{\det B_0}{\det \Phi(e^{i\lambda}) \det \Pi(e^{-i\lambda})}.$$

By construction, $\Pi(z) = I_2 - \Pi_1 z$ has determinant $\det[\Pi(z)] = 1 - \rho z$, with unique root $z = 1/\rho$. Under Assumption (A1), $|\rho| < 1$ implies $|1/\rho| > 1$, so $\det[\Pi(e^{-i\lambda})] = 1 - \rho e^{-i\lambda} \neq 0$ for all $\lambda$.

The noncausal polynomial $\Phi(z)$ inherits its lower-triangular structure from the coefficient matrices $\Phi_j$, so

$$\det[\Phi(z)] = \left(1 - \sum_{j=1}^{s} \phi_{j,11} z^j\right) \cdot 1.$$

When $\chi = 0$, all $\phi_{j,11} = 0$ and $\det[\Phi(z)] = 1$ identically. When $0 < \chi < 1$, the expansion $(1+\chi z^l)^{-1}$ and Assumption (A3) imply that the scalar polynomial $1 - \sum_{j=1}^{s} \phi_{j,11} z^j$ has no zeros on or inside the unit circle. In particular, the roots of the denominator of $(1 + \chi z^l)$ lie strictly outside the unit circle, so the truncated approximation inherits invertibility on $|z| \leq 1$ for sufficiently large $s$. Hence $\det[\Phi(e^{i\lambda})] \neq 0$ for all $\lambda$.

Finally, $\det B_0 = 1$ by construction. Combining these results, we obtain

$$\det[\varphi(\lambda)] = \frac{1}{\det \Phi(e^{i\lambda}) \det \Pi(e^{-i\lambda})} \neq 0 \quad \forall \lambda \in [-\pi, \pi].$$

Therefore, $\operatorname{rank}[\varphi(\lambda)] = 2 = n_u$ for all $\lambda$, which satisfies the recoverability condition of Chahrour and Jurado (2021). □

**Corollary A1.** *Under the conditions of Proposition A3, the structural shocks can be recovered explicitly as*

$$u_t = B_0^{-1}\Pi(L)\Phi(L^{-1})y_t, \tag{A26}$$

*which is a finite linear combination of leads and lags of the observables. In particular,*

$$\begin{bmatrix} \epsilon_{t-l} \\ \nu_t \end{bmatrix} = \begin{bmatrix} 1 & 0 \\ 1 & 1 \end{bmatrix} \left( y_t - \Pi_1 y_{t-1} - \sum_{j=1}^{l} \Phi_j y_{t+j} \right).$$

The corollary illustrates how the noncausal representation resolves the recoverability problem: the news shock can be expressed as a projection of the structural innovation onto a finite number of leads and lags of the observable process. In contrast, a purely causal representation would necessarily fail to span the news shock whenever $\chi < 1$.

# C Data

This appendix summarises the variables used in the empirical analysis, together with their sources and transformations. The full list of series, data providers, and construction details is reported in Table C. The baseline four-variable system comprises the percentage change in world oil production, a proxy for global real economic activity, the real oil price, and the percentage change in global oil stocks. Additional macroeconomic and financial variables are documented in the same table.

Table A1: Variables used, sources and transformations

| Variables | Code | Period | Data source | Transformation |
|---|---|---|---|---|
| **Global Oil Market Variables** | | | | |
| World oil production | WOP | 1974:01-2025:07 | US EIA's Monthly Energy Review | First log difference |
| World industrial production | WIP | 1974:01-2025:07 | Christiane Baumeister website | First log difference |
| Refiner acquisition cost | RAC | 1974:01-2025:07 | US EIA's Monthly Energy Review | Level |
| World oil stocks[a] | Stocks | 1974:01-2025:07 | US EIA's Monthly Energy Review | First difference |
| **Global economic variable** | | | | |
| Global Economic Conditions indicators | GECON | 1974:01-2025:07 | Christiane Baumeister website | Level |
| Geopolitical Risk Index | GPR | 1974:01-2025:07 | Caldara et al. (2019) | Level |
| OECD Inflation | Infl_OECD | 1974:01-2025:02 | OECD database | Level |
| OECD passenger car registrations | PCR_OECD | 1974:01-2019:1 | OECD database | Level |
| World stock price index | MSCI | 1974:01-2025:07 | Datastream | First log difference |
| **US macroeconomic variables** | | | | |
| Consumer price index for all urban consumers and all items | CPI | 1974:01-2025:07 | FRED Database | First log difference |
| Consumer price index for all urban consumers: Energy in U.S. City Average | CPIENG | 1974:01-2025:07 | FRED Database | First log difference |
| Consumer price index excluding food and energy | Core CPI | 1974:01-2025:07 | FRED Database | First log difference |
| Producer Price Index | PPIACO | 1974:01-2025:07 | FRED Database | First log difference |
| US Industrial production | INDPROD | 1974:01-2025:07 | FRED Database | First log difference |
| US Unemployment rate | UNRATE | 1974:01-2025:07 | FRED Database | Level |
| University of Michigan: Inflation Expectation | INF_EXP | 1978:01-2025:07 | Michigan Survey | Level |
| Business Tendency Surveys for Manufacturing | BSCI | 1974:01-2025:07 | FRED Database | Level |
| 1-Year Ahead Macroeconomic Uncertainty[b] | Macro_uncertainty | 1974:01-2025:07 | FRED Database | Level |
| Long-term interest rate | 10Y GB | 1974:01-2025:07 | FRED Database | Level |
| Stock price index | SP500 | 1974:01-2025:07 | Bloomberg | First log difference |
| Real effective exchange rate | REER | 1974:01-2025:07 | FRED Database | First log difference |

[a] Following Kilian and Murphy (2014)'s method, the world oil stock variable is constructed by rescaling U.S. crude oil inventories with the OECD-to-U.S. petroleum stocks ratio. All variables are from the EIA database and the series is seasonally adjusted.

[b] Macroeconomic uncertainty is proxied by 12-month ahead macro uncertainty measure of Jurado et al. (2015), drawn from large number of U.S. macroeconomic time series.

# D Bayesian estimation of the noncausal VAR

This appendix provides a detailed account of the Bayesian estimation procedure for the NC-VAR$(r, s)$ model used in the empirical analysis. The algorithm closely follows Lanne and Luoto (2016) and Nelimarkka (2017a), exploiting the conditional normality of the likelihood under the multivariate $t$-distribution assumption and combining it with Minnesota-

type priors designed to stabilize the posterior and favor parsimonious dynamics, especially on the noncausal side.

## D.1 Model setup and notation

Recall the NC-VAR($r$,$s$) model

$$\Pi(L)\Phi(L^{-1})y_t = \epsilon_t$$

where $\Pi(L) = I_n - \Pi_1 L - \cdots - \Pi_r L^r$ is the causal polynomial, $\Phi(L^{-1}) = I_n - \Phi_1 L^{-1} - \cdots - \Phi_s L^{-s}$ is the noncausal polynomial, and $\epsilon_t$ follows a multivariate $t$-distribution as in equation (11):

$$\epsilon_t = \omega_t^{-1/2}\eta_t, \quad \eta_t \sim \mathcal{N}(0,\Sigma), \quad \lambda\omega_t \sim \chi^2_\lambda$$

The scalar factor $\omega_t^{-1/2}$ introduces time-varying volatility and generates fat tails when $\lambda$ is small.

Let $\Pi$ and $\Phi$ denote the matrices obtained by stacking $\Pi_i'$ for $i = 1,\ldots,r$ and $\Phi_i'$ for $i = 1,\ldots,s$, respectively. Denote $\pi = \text{vec}(\Pi)$, $\phi = \text{vec}(\Phi)$, and collect the parameters in $\theta = (\pi', \phi', \text{vech}(\Sigma)', \lambda)'$. For convenience, write $\vartheta = (\pi', \phi')'$. To impose $s^*$ zero restrictions on $\Phi$, we introduce an $((n^2s - s^*)\times 1)$ vector $\phi_r$ containing the unrestricted lead coefficients, together with a deterministic selection matrix $R_\phi$ of dimension $n^2s \times (n^2s - s^*)$ such that $\phi = R_\phi \phi_r$. When no restrictions are imposed, $R_\phi = I_{n^2s}$ and $\phi_r = \phi$.

## D.2 Conditional likelihood

Define the auxiliary variables:

$$v_t(\phi) = y_t - \Phi_1 y_{t+1} - \cdots - \Phi_s y_{t+s}$$

and the transformed error:

$$\epsilon_t(\vartheta) = v_t(\phi) - \sum_{j=1}^{r} \Pi_j v_{t-j}(\phi)$$

The approximate conditional joint density of $y = (y_1,\ldots,y_T)$ given $\omega = (\omega_{r+1},\ldots,\omega_{T-s})$ is:

$$p(y|\omega,\theta) \approx \prod_{t=r+1}^{T-s} p(\epsilon_t(\vartheta)|\omega_t,\Sigma)$$

where

$$p(\epsilon_t|\omega_t,\Sigma) = \frac{\omega_t^{n/2}}{(2\pi)^{n/2}|\Sigma|^{1/2}} \exp\left(-\frac{1}{2}\omega_t \epsilon_t(\vartheta)'\Sigma^{-1}\epsilon_t(\vartheta)\right)$$

## D.3 Prior distributions

We adopt Minnesota-type priors on the lag and lead coefficients and standard conjugate priors on the covariance matrix, combined with an exponential prior on the degrees of freedom. Specifically,

$$\begin{aligned}
\pi &\sim \mathcal{N}(\underline{\pi}, V_\pi) \cdot \mathbf{1}(\pi) \\
\phi_r &\sim \mathcal{N}(\underline{\phi}_r, V_{\phi_r}) \cdot \mathbf{1}(\phi), \quad \phi = R_\phi \phi_r \\
\Sigma &\sim \mathcal{IW}(\underline{S}, \underline{\nu}) \\
\lambda &\sim \text{Exp}(\underline{\lambda})
\end{aligned}$$

where $\mathbf{1}(\cdot)$ is an indicator function equal to one when the associated polynomial has all roots outside the unit circle, and $\mathcal{IW}$ denotes the inverse Wishart distribution. The prior means on the dynamic coefficients are set to zero: $\underline{\pi} = 0$ and $\underline{\phi}_r = 0$, while the prior covariance matrices $V_\pi$ and $V_{\phi_r}$ are diagonal with elements:

$$\begin{aligned}
\sigma_{\pi,iil} &= \frac{\gamma_{1,\pi}}{l^{\gamma_3}}, \quad \sigma_{\pi,ijl} = \gamma_2 \frac{\gamma_{1,\pi}}{l^{\gamma_3}} \frac{\hat{\sigma}_i}{\hat{\sigma}_j}, \quad i,j = 1,\dots,n, \quad l = 1,\dots,r \\
\sigma_{\phi_r,iil} &= \frac{\gamma_{1,\phi}}{l^{\gamma_3}}, \quad \sigma_{\phi_r,ijl} = \gamma_2 \frac{\gamma_{1,\phi}}{l^{\gamma_3}} \frac{\hat{\sigma}_i}{\hat{\sigma}_j}, \quad i,j = 1,\dots,n, \quad l = 1,\dots,s
\end{aligned}$$

where $\hat{\sigma}_i$ is the residual standard error from a univariate autoregression on the $i$th variable with $r$ lags, $\gamma_{1,\pi}$ and $\gamma_{1,\phi}$ control overall tightness, $\gamma_2$ controls the relative tightness of cross-lag coefficients, and $\gamma_3$ governs the decay variance with lag length. In our baseline, we set $\gamma_{1,\pi} = 0.2$, $\gamma_{1,\phi} = 0.15$, $\gamma_{2,\pi} = 0.5$, $\gamma_{2,\phi} = 0.5$, $\gamma_{3,\pi} = 1.2$ and $\gamma_{3,\phi} = 1$. The tighter prior on leads ($\gamma_{1,\phi} < \gamma_{1,\pi}$) reflects the view that noncausal terms should be present only when supported by the data and helps to stabilize the posterior by shrinking lead coefficients more aggressively towards zero. This asymmetric shrinkage is crucial to achieving unimodality of the posterior distribution.

For the covariance matrix, we choose $\underline{S} = (\underline{\nu} - n - 1)\,\text{diag}(\hat{\sigma}_1^2, \dots, \hat{\sigma}_n^2)$ with $\underline{\nu} = n + 2$, so that the prior mean of $\Sigma$ coincides with the diagonal matrix of univariate residual variances. The prior mean of the degrees-of-freedom parameter is set via $\underline{\lambda} = 8$, which corresponds to a relatively light-tailed prior; as shown in the empirical section, the posterior mean of $\lambda$ is much lower, indicating that the data strongly favor fat tails.

## D.4 Gibbs sampler

The posterior distribution of $\theta$ is simulated using a Gibbs sampler with a Metropolis–Hastings step for $\lambda$. Let $t$ range from $r + 1$ to $T - s$. For each draw, we proceed as follows.

**Step 1: Draw $\phi_r$.** Define

$$v_t^*(\phi) = \omega_t^{1/2}\Pi(L)y_t, \qquad X_t^* = \omega_t^{1/2}\Pi(L)\begin{bmatrix} y_{t+1}' & \cdots & y_{t+s}' \end{bmatrix}'.$$

Stacking across $t$ yields $Y^*$ and $X^*$. The conditional posterior of $\phi_r$ is Gaussian:

$$\phi_r|y,\pi,\Sigma,\omega \sim \mathcal{N}(\bar{\phi}_r, \bar{V}_{\phi_r})\,\mathbf{1}(\phi), \qquad \phi = R_\phi\phi_r,$$

with

$$\begin{aligned}\bar{V}_{\phi_r}^{-1} &= V_{\phi_r}^{-1} + R_\phi' X^{*\prime}\Omega X^* R_\phi,\\ \bar{\phi}_r &= \bar{V}_{\phi_r}\left(V_{\phi_r}^{-1}\underline{\phi}_r + R_\phi' X^{*\prime}\Omega Y^*\right),\end{aligned}$$

where $\Omega = I_{T-r-s}\otimes\Sigma^{-1}$.

**Step 2: Draw $\pi$.** Let $v_t(\phi)$ be as above and define

$$Y = \begin{bmatrix} v_{r+1}(\phi)' \\ \vdots \\ v_{T-s}(\phi)' \end{bmatrix}, \qquad U = \begin{bmatrix} v_r(\phi)' & \cdots & v_1(\phi)' \\ \vdots & \ddots & \vdots \\ v_{T-s-1}(\phi)' & \cdots & v_{T-s-r}(\phi)' \end{bmatrix}.$$

The conditional posterior for $\pi$ is

$$\pi|y,\phi,\Sigma,\omega \sim \mathcal{N}(\bar{\pi}, \bar{V}_\pi)\,\mathbf{1}(\pi),$$

with

$$\begin{aligned}\bar{V}_\pi^{-1} &= V_\pi^{-1} + \Sigma^{-1}\otimes U'U,\\ \bar{\pi} &= \bar{V}_\pi\left(V_\pi^{-1}\underline{\pi} + \mathrm{vec}(U'Y\Sigma^{-1})\right).\end{aligned}$$

**Step 3: Draw $\Sigma$.** Defining $E = Y - U\Pi$ and $\bar{S} = \underline{S} + E'E$, $\bar{\nu} = \underline{\nu} + T - s - r$, the conditional posterior is inverse-Wishart:

$$\Sigma|y,\pi,\phi,\omega \sim \mathcal{IW}(\bar{S},\bar{\nu}).$$

**Step 4: Draw $\omega_t$.** For each $t = r+1,\ldots,T-s$, the conditional distribution of $\omega_t$ is chi-squared:

$$\left(\lambda + \epsilon_t(\vartheta)'\Sigma^{-1}\epsilon_t(\vartheta)\right)\omega_t \,\Big|\, y,\pi,\phi,\Sigma,\lambda \sim \chi^2_{\lambda+n}.$$

**Step 5: Draw $\lambda$.** The degrees-of-freedom parameter is updated using a Metropolis–Hastings step with proposal centered at the mode of the conditional posterior. The

kernel of the conditional density is proportional to

$$p(\lambda|y,\omega) \propto \left(2^{\lambda/2}\Gamma(\lambda/2)\right)^{-(T-r-s)} \lambda^{\lambda(T-r-s)/2} \left(\prod_{t=r+1}^{T-s} \omega_t^{(\lambda-2)/2}\right) \exp\left[-\left(\frac{1}{\underline{\lambda}} + \frac{1}{2}\sum_{t=r+1}^{T-s} \omega_t\right)\lambda\right].$$

A univariate normal proposal, with mean equal to the mode and variance equal to the inverse of the second derivative of the log-kernel, is used to generate candidate values of $\lambda$, which are then accepted or rejected according to the usual Metropolis–Hastings rule.

### D.5 Posterior inference

In the empirical application, we run the Gibbs sampler for a sufficiently long burn-in period (50,000 iterations) and retain 10,000 draws for posterior inference. For each retained draw $(\pi^{(m)}, \phi^{(m)}, \Sigma^{(m)}, \lambda^{(m)})$, $m = 1, \ldots, 10000$, we compute the two-sided MA coefficients $\{\Psi_h^{(m)}\}_{h=-s}^{H}$ implied by equation (9), perform the Max-Share identification to obtain the rotation matrix $W^{(m)}$, and construct the structural impulse responses $\Theta_h^{(m)} = \Psi_h^{(m)} \tilde{A}^{(m)} W^{(m)}$. Reported impulse responses are posterior medians, and the accompanying credible sets correspond to the relevant posterior quantiles.

The posterior distribution of the degrees-of-freedom parameter $\lambda$ provides a useful diagnostic for the relevance of non-Gaussianity. In our baseline specification, the posterior mass is concentrated around values below 5, with negligible probability above 6, as illustrated in Figure A1. This strong evidence of fat tails corroborates the use of a multivariate $t$-distribution and ensures uniqueness of the NC-VAR representation.

## E Validation of the noncausal VAR specification

This section gathers additional evidence in favor of the noncausal VAR specification employed in the main analysis. We focus on two complementary aspects: the posterior distribution of the degrees-of-freedom parameter, which informs the role of non-Gaussianity in identification, and the lag/lead selection procedure, which documents the empirical relevance of noncausal dynamics.

### E.1 Evidence from the estimated degrees of freedom

Figure A1 plots the posterior density of the degrees-of-freedom parameter $\lambda$ for the baseline four-variable NC-VAR$(12, 12)$ model. The histogram and kernel estimate show that the posterior distribution is sharply concentrated at low values, with a mode around 3–4 and virtually no mass beyond 6. Given that the prior mean is centered around 8, this indicates that the data strongly favor fat-tailed innovations and decisively reject Gaussianity.

The non-Gaussian assumption is therefore not a technical convenience but an empirically supported feature that underpins the uniqueness of the NC-VAR representation.

Figure A1: Posterior density of DOF parameter $\lambda$

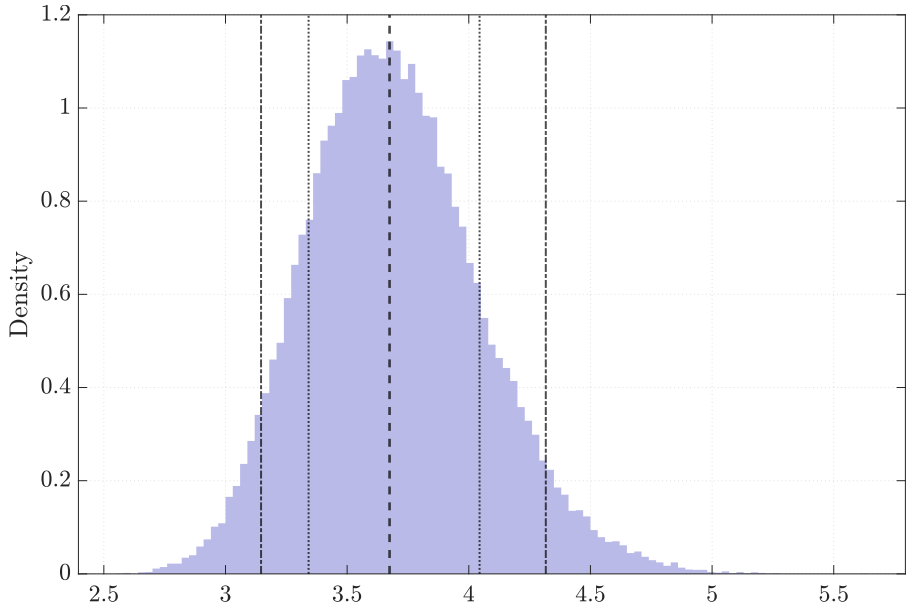


Notes: The figure reports the posterior distribution of the degrees-of-freedom parameter $\lambda$ for the four-variable NC-VAR(12,12) model. Blue bars indicate the histogram of posterior draws; the solid line denotes the associated kernel density estimate.

## E.2 Model lag and lead delection procedure

We next document the lag-selection procedure used to assess whether the data favor a purely causal or a genuinely noncausal representation. For each total order $p = r + s$, we estimate causal VAR($p$) models and NC-VAR($r, s$) models with different allocations of lags and leads. Model comparison is based on standard information criteria and on the log marginal likelihood, with particular emphasis on whether best-performing specifications include noncausal terms.

### E.2.1 Step 1: Total lag order selection

Table A2 reports the Akaike Information Criterion (AIC) for causal VAR($p$) models with $p$ ranging from 1 to 24. The AIC favors $p = 7$ as the preferred total lag order, which serves as a benchmark for the subsequent decomposition into causal and noncausal components.

Table A2: Lag length selection for causal VAR($p$)

| $p$ | 1 | 2 | 3 | 4 | 5 | 6 | 7 | 8 | 9 | 10 | 11 | 12 |
|---|---|---|---|---|---|---|---|---|---|---|---|---|
| AIC | 2859 | 2662 | 2617 | 2613 | 2604 | 2602 | **2594**$^*$ | 2612 | 2629 | 2625 | 2623 | 2594 |
| $p$ | 13 | 14 | 15 | 16 | 17 | 18 | 19 | 20 | 21 | 22 | 23 | 24 |
| AIC | 2602 | 2604 | 2610 | 2624 | 2622 | 2634 | 2642 | 2638 | 2614 | 2622 | 2616 | 2614 |

Notes: The table reports the Akaike Information Criterion (AIC) for causal VAR($p$) models estimated on the baseline four-variable system. The star * indicates the order $p = 7$ that minimises the AIC. Sample size: $T = 618$.

### E.2.2 Step 2: Causal versus noncausal specification

Given the preferred total order $p = 7$, Table A3 compares alternative NC-VAR($r, s$) specifications with $r + s = 7$ using both the log marginal likelihood and the AIC. The best-performing model in terms of marginal likelihood is a noncausal specification with $r = 3$ lags and $s = 4$ leads. The AIC, in turn, favours another noncausal model with $r = 1$ and $s = 6$. A purely causal VAR(7) is dominated by several noncausal alternatives, with Bayes factors well below 0.1 relative to the best model.

Table A3: Bayesian Model Comparison: VAR($r, s$) with $r + s = 7$

| Rank | $r$ | $s$ | Log ML | $\Delta$ Log ML | Bayes Factor | AIC | Type |
|---|---|---|---|---|---|---|---|
| 1 | 3 | 4 | -993.28 | 0.00 | 1.0000 | 2087.03 | Noncausal |
| 2 | 5 | 2 | -997.88 | -4.60 | 0.0100 | 2161.87 | Noncausal |
| 3 | 6 | 1 | -1008.48 | -15.20 | 2.51e-07 | 2214.16 | Noncausal |
| 4 | 4 | 3 | -1022.42 | -29.14 | 2.21e-13 | 2179.52 | Noncausal |
| 5 | 7 | 0 | -1022.50 | -29.22 | 2.04e-13 | 2273.40 | Causal |
| 6 | 1 | 6 | -1024.55 | -31.27 | 2.62e-14 | 2085.35* | Noncausal |
| 7 | 2 | 5 | -1025.68 | -32.40 | 8.50e-15 | 2122.07 | Noncausal |

Notes: Log ML denotes the log marginal likelihood computed via the Harmonic Mean Estimator (HME) with 5% trimming. $\Delta$ Log ML is the difference relative to the best model. Bayes Factor is computed as exp($\Delta$Log ML) relative to the best model. A Bayes Factor below 1/10 (i.e., $\Delta$ Log ML $< -2.30$) indicates strong evidence against the model. AIC denotes the Akaike Information Criterion; * indicates the model with the lowest AIC. Best model (Log ML): VAR(3,4). Best model (AIC): VAR(1,6).

## E.3 Moving restrictions on real economic activity

Figure A2: Impulse response functions to oil news shocks without restrictions on WIP

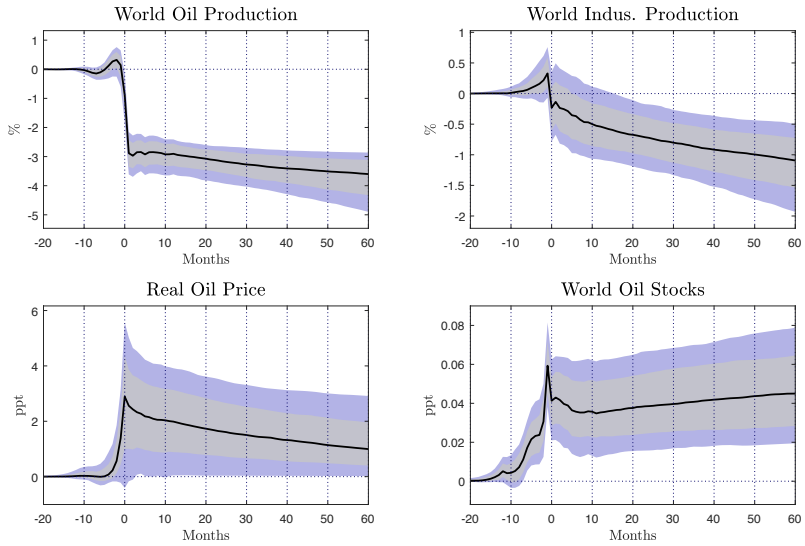


The figure displays posterior median impulse responses and associated 68 % and 90 % credible sets. Solid lines and shaded areas correspond to the earlier period, while dashed and dotted lines represent the later period. Owing to noncausality, impulse responses are defined on both sides of zero, with negative horizons capturing the lead terms of the NC-VAR moving-average representation.

Figure A2 reports the impulse response functions obtained after relaxing all zero restrictions (i.e., $R_\phi = I_{n^2 s}$). The qualitative pattern of responses is largely preserved, indicating that the main findings survive when the identifying restrictions are relaxed.

## E.4 Alternative truncation windows

Figure A3: News shock identification with different truncation windows ($H_1$; $H_2$)

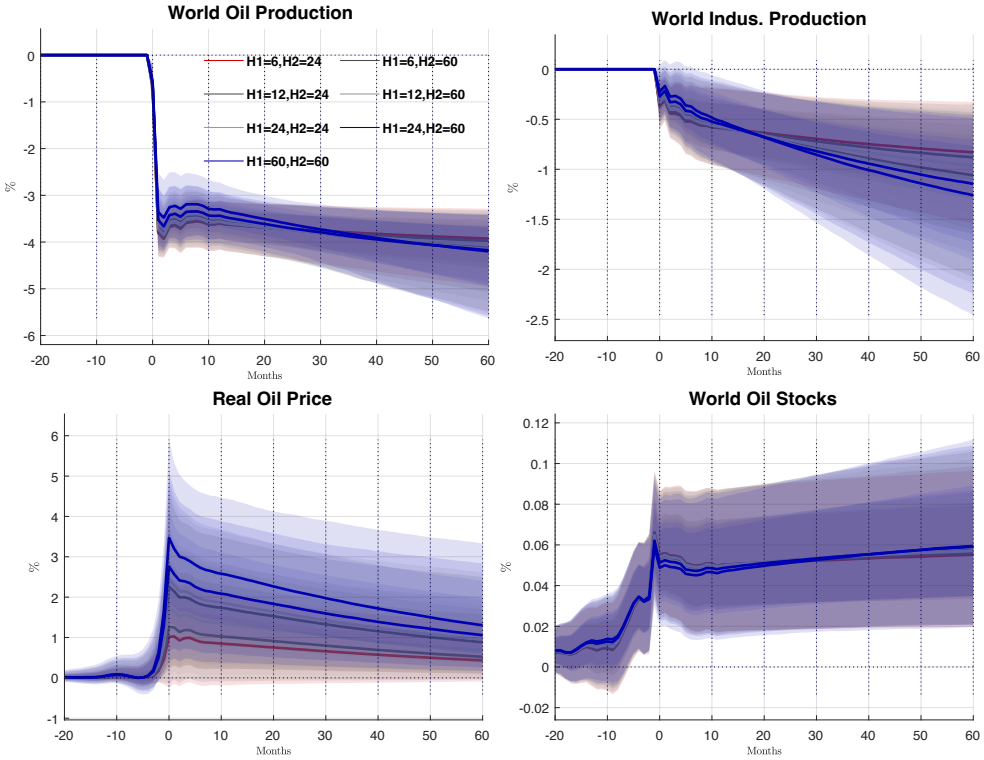


Notes: The black dashed lines are the posterior median responses of the 4-variable baseline model. The solid lines are the posterior median cumulated impulse responses of the NC-VAR(6,6). Light and dark grey shaded regions are the 90 % and 68 % credible sets of the NC-VAR(12,12). Because of noncausality, the impulse responses are located on both sides of zero. The negative side corresponds to the lead terms of the MA representation of NC-VAR.

## E.5 Time backtest

Figure A4: Impulse response functions to oil news shocks across different sub-samples.

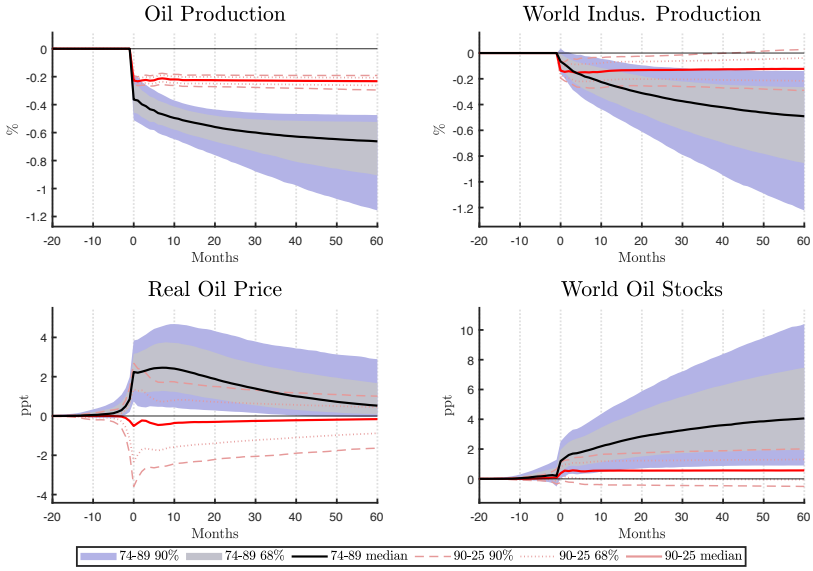


The figure displays posterior median impulse responses and associated 68 % and 90 % credible sets for the 1974–1989 and 1990–2025 samples. Black solid lines and shaded areas correspond to the earlier period, while red dashed and dotted lines represent the later period. Owing to noncausality, impulse responses are defined on both sides of zero, with negative horizons capturing the lead terms of the NC-VAR moving-average representation.

## E.6 Noncausal vs causal VAR

Figure A5: Impulse-response functions to the identified oil supply news shock: NC-VAR versus causal VAR

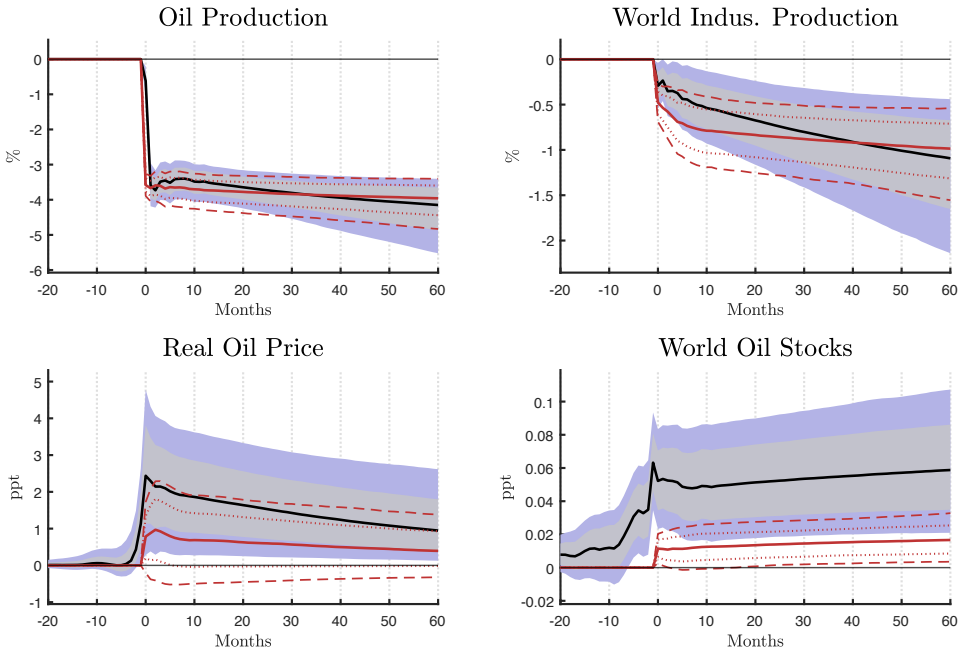


*Notes:* The figure compares the impulse responses obtained from the baseline NC-VAR(12,12) specification and from a purely causal VAR(12) benchmark following the same max-share identification strategy. Black solid lines denote the posterior median responses of the NC-VAR(12,12), while shaded areas represent the associated 90% and 68% credible sets. Red dashed and dotted lines correspond respectively to the 90% and 68% credible sets of the causal VAR(12), and red solid lines denote the posterior median responses. Responses are normalized to a negative oil production shock. Because of noncausality, the NC-VAR impulse responses are defined on both sides of zero. Negative horizons correspond to the lead terms of the bilateral moving-average representation and capture anticipatory dynamics that are absent from the causal VAR specification.

# F Historical decomposition: causal vs. non-causal estimates

Figure A6: Contribution of oil supply news shocks to real oil price

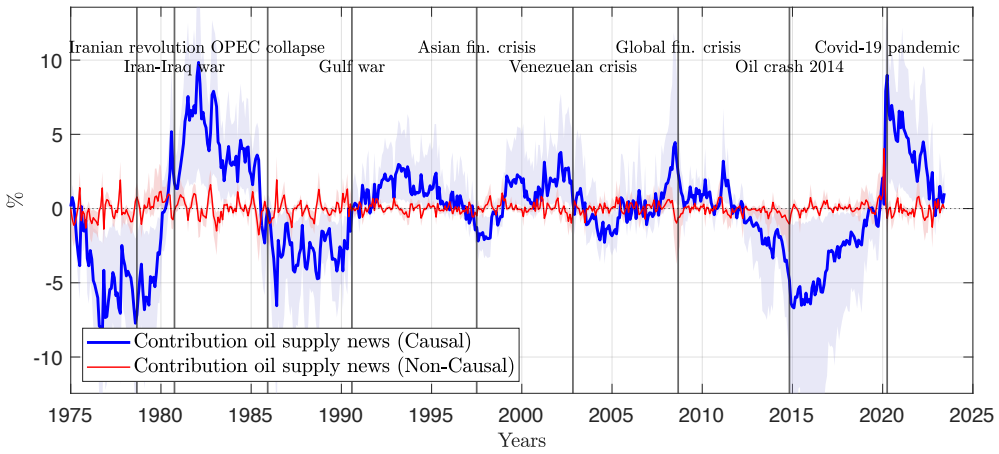


*Notes:* The figure displays the posterior median contribution of oil supply news shocks to real oil price fluctuations under causal (blue) and non-causal (red) specifications. Shaded areas denote the associated 90% credible intervals. Vertical lines mark major oil market events.

# G IRFs under the OPEC and Non-OPEC oil production distinction

## G.1 Reactions of global macroeconomic variables

Figure A7: Reactions of global macroeconomic variables to a OPEC news shock

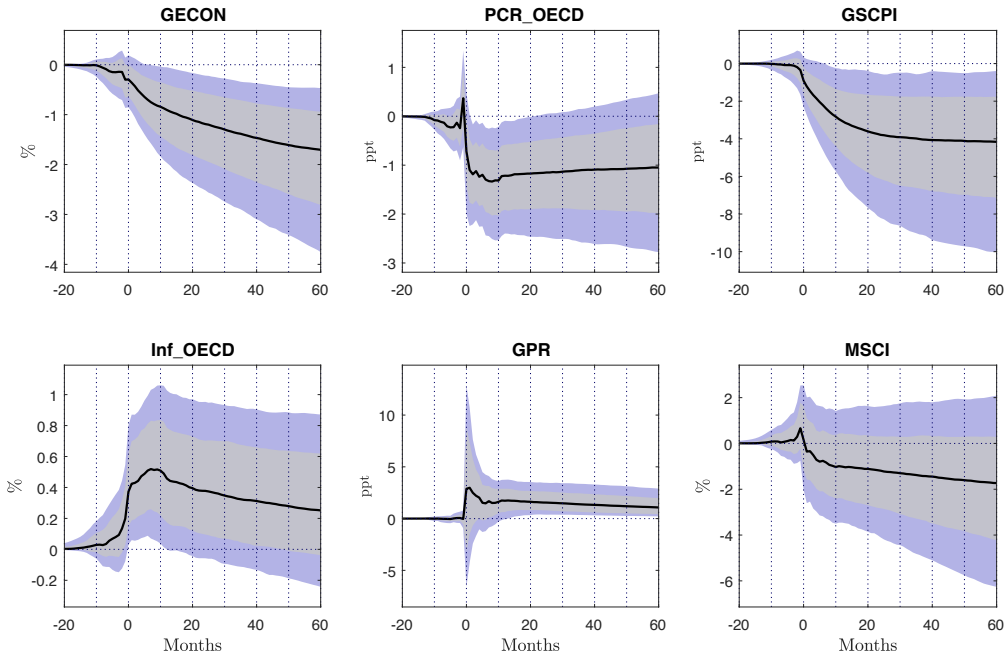


Notes: The solid lines are the posterior median cumulated impulse responses of global macroeconomics variables. Blue and grey shaded areas are the 90 and 68 % credible sets of the NC-VAR(12,12). Because of noncausality, the impulse responses are located on both sides of zero. The negative side corresponds to the lead terms of the MA representation.

Figure A8: Reactions of global macroeconomic variables to a NON-OPEC news shock

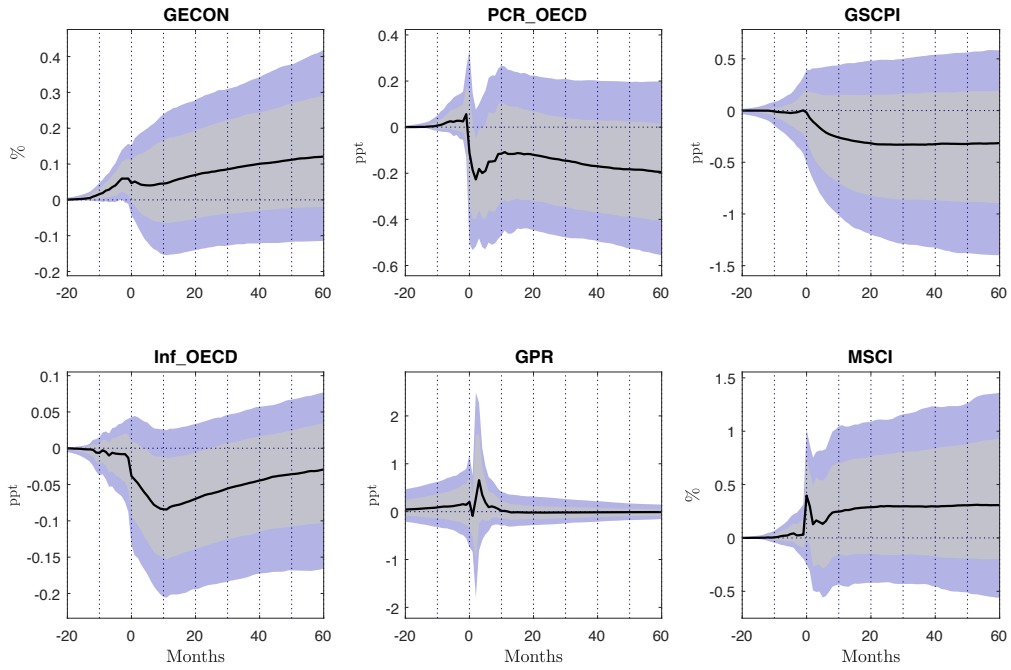


Notes: The solid lines are the posterior median cumulated impulse responses of global macroeconomics variables. Blue and grey shaded areas are the 90 and 68 % credible sets of the NC-VAR(12,12). Because of noncausality, the impulse responses are located on both sides of zero. The negative side corresponds to the lead terms of the MA representation.

## G.2 Reactions of US macroeconomic variables

Figure A9: Reactions of US macroeconomic variables to a OPEC supply news shock

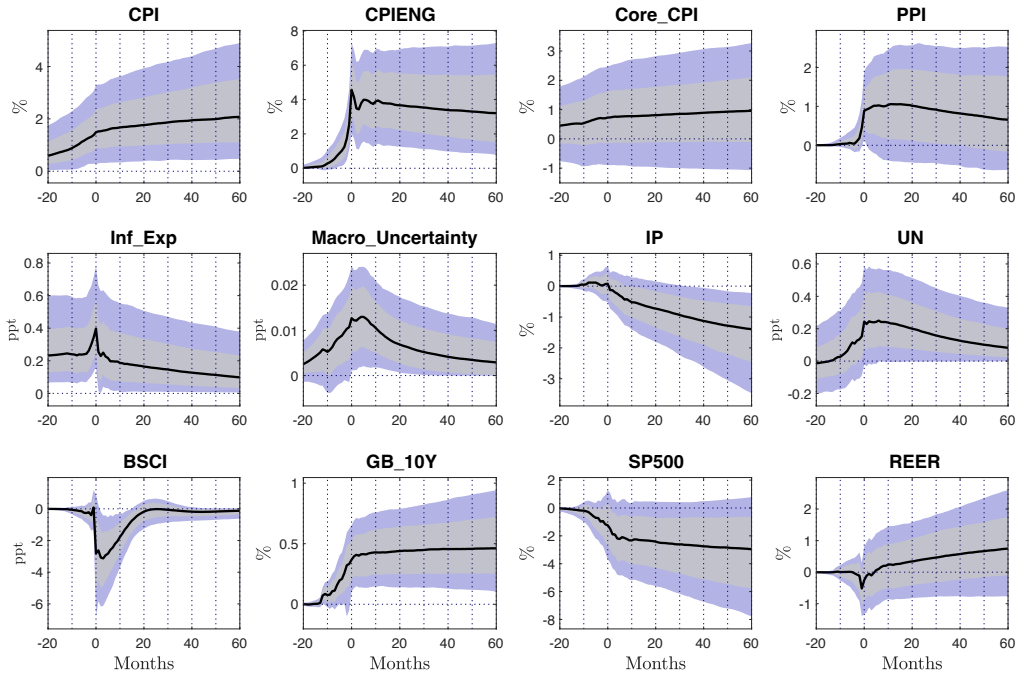


Notes: The solid lines are the posterior median cumulated impulse responses of US macroeconomics variables. Blue and grey shaded areas are the 90 and 68 % credible sets of the NC-VAR(12,12). Because of noncausality, the impulse responses are located on both sides of zero. The negative side corresponds to the lead terms of the MA representation.

Figure A10: Reactions of US macroeconomic variables to a Non-OPEC news shock

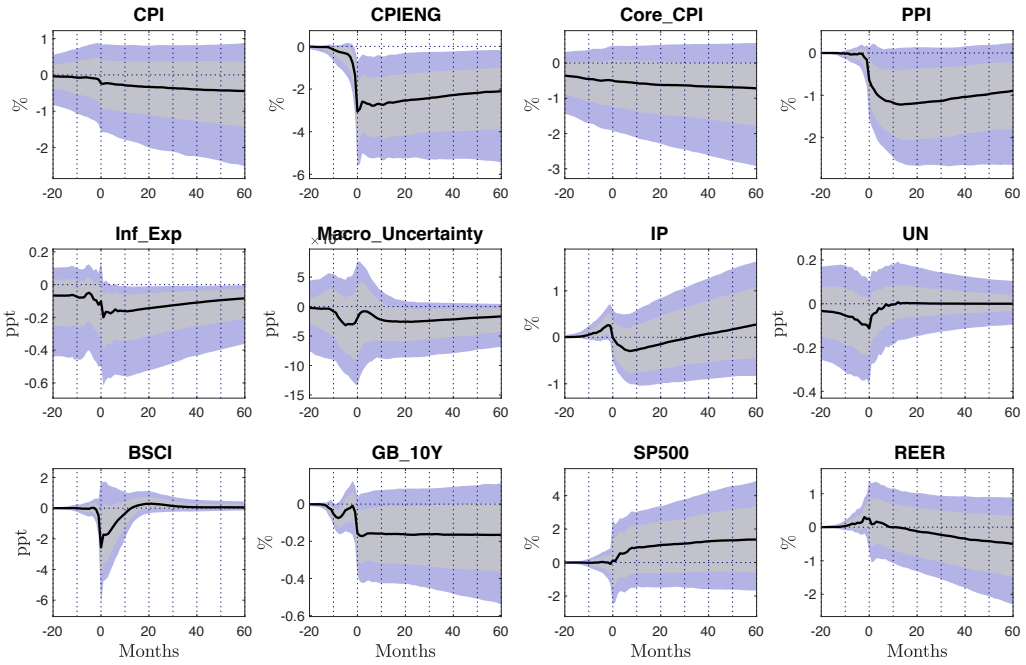


Notes: The solid lines are the posterior median cumulated impulse responses of US macroeconomics variables. Blue and grey shaded areas are the 90 and 68 % credible sets of the NC-VAR(12,12). Because of noncausality, the impulse responses are located on both sides of zero. The negative side corresponds to the lead terms of the MA representation.

# References


Caldara, D., Cavallo, M., Iacoviello, M., 2019. Oil price elasticities and oil price fluctuations. Journal of Monetary Economics 103, 1–20.

Chahrour, R., Jurado, K., 2021. Recoverability and expectations-driven fluctuations. The Review of Economic Studies 89, 214–239.

Davis, R.A., Song, L., 2020. Noncausal vector ar processes with application to economic time series. Journal of Econometrics 216, 246–267.

Giancaterini, F., 2023. Essays on Univariate and Multivariate Noncausal Processes. Doctoral dissertation. Maastricht University.

Gourieroux, C., Jasiak, J., 2017. Noncausal vector autoregressive process: Representation, identification and semi-parametric estimation. Journal of Econometrics 200, 118–134.

Jurado, K., Ludvigson, S.C., Ng, S., 2015. Measuring uncertainty. American Economic Review 105, 1177–1216.

Kilian, L., Murphy, D.P., 2014. The role of inventories and speculative trading in the global market for crude oil. Journal of Applied Econometrics 29, 454–478.

Lanne, M., Luoto, J., 2016. Noncausal bayesian vector autoregression. Journal of Applied Econometrics 31, 1392–1406.

Lanne, M., Saikkonen, P., 2013. Noncausal Vector Autoregression. Econometric Theory 29, 447–481.

Nelimarkka, J., 2017. Evidence on News Shocks under Information Deficiency. MPRA Paper 80850. University Library of Munich, Germany.